Electronic Supporting Information

Magnetism of transition-metal doped tetrel nanoclusters: Multi-reference character and spin-orbit effects

Jannik Mehmel,* Carlos M. Jimenez-Muñoz, Filip Rivic, Vera Krewald, and Rolf Schäfer

Technical University of Darmstadt, Eduard-Zintl-Institute, Peter-Grünberg-Straße 8, 64287 Darmstadt, Germany.

---

1 Electric Deflection Experiments

In Fig. S1 the electric deflection profiles are shown for the $Sn_{12}TM$ clusters with TM = Mn, Cr, Fe at a nozzle temperature of $T_{\mathrm{nozzle}} = 16$ K and a deflection voltage of $U = 24$ kV. In short, the deflection of the clusters depends on the electronic polarizability and the permanent electric dipole moment, the latter being the structure-sensitive property. For rigid clusters, the presence of a permanent dipole moment leads to a broadening of the molecular beam. In contrast, the polarizability causes a single-sided shift of the molecular beam.

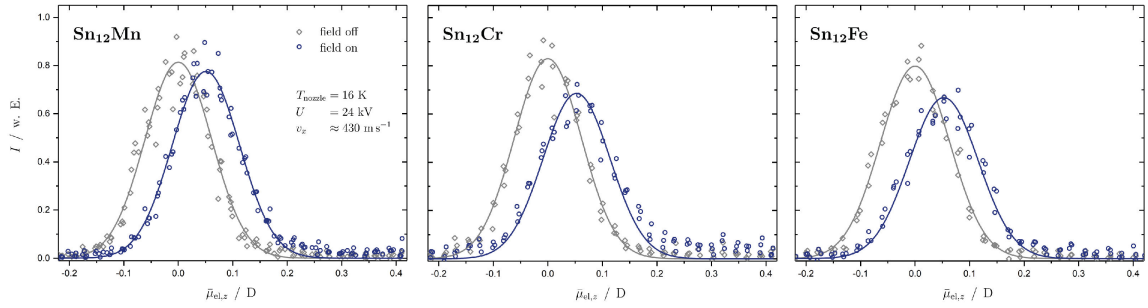

Figure S1. Electric deflection profiles of $Sn_{12}TM$ with TM = Mn, Cr, Fe (from left to right) at $T_{\mathrm{nozzle}} = 16$ K and a deflection voltage of $U = 24$ kV. The intensity I is given as a function of the projection of the observed electric dipole moment on the field direction averaged over the length of the deflection unit $\bar{\mu}_{\mathrm{el},z}$. The grey squares represent the cluster intensity without applied field whereas blue open circles represent the intensity with applied electric field. Gaussian functions are fitted to the experimental data without (grey solid line) and with applied electric field (blue solid line). The width of the latter is equal to the fit function of the experimental data without field, since no beam broadening is observed for the majority of points.

It can be seen that the intensity in the beam center is depicted very well by the Gaussian fit function. However, a small tailing in the direction of the field gradient can be seen which is not described by the Gaussian. As was demonstrated in a previous study on $Sn_{12}X$ clusters with X = Al, Ga and In, the deflection profiles can be explained by the presence of two fractions of clusters, i.e. one being nonpolar suggesting an inversion center to be present in the structure and one being polar and less symmetric. Since the polar fraction is very small compared to the nonpolar fraction, we are only focussed on this nonpolar isomer which is a spherical rotor.

*Corresponding author: jannik.mehmel@wihi.tu-darmstadt.de

2 Temperature-dependent Magnetic Deflection Experiments

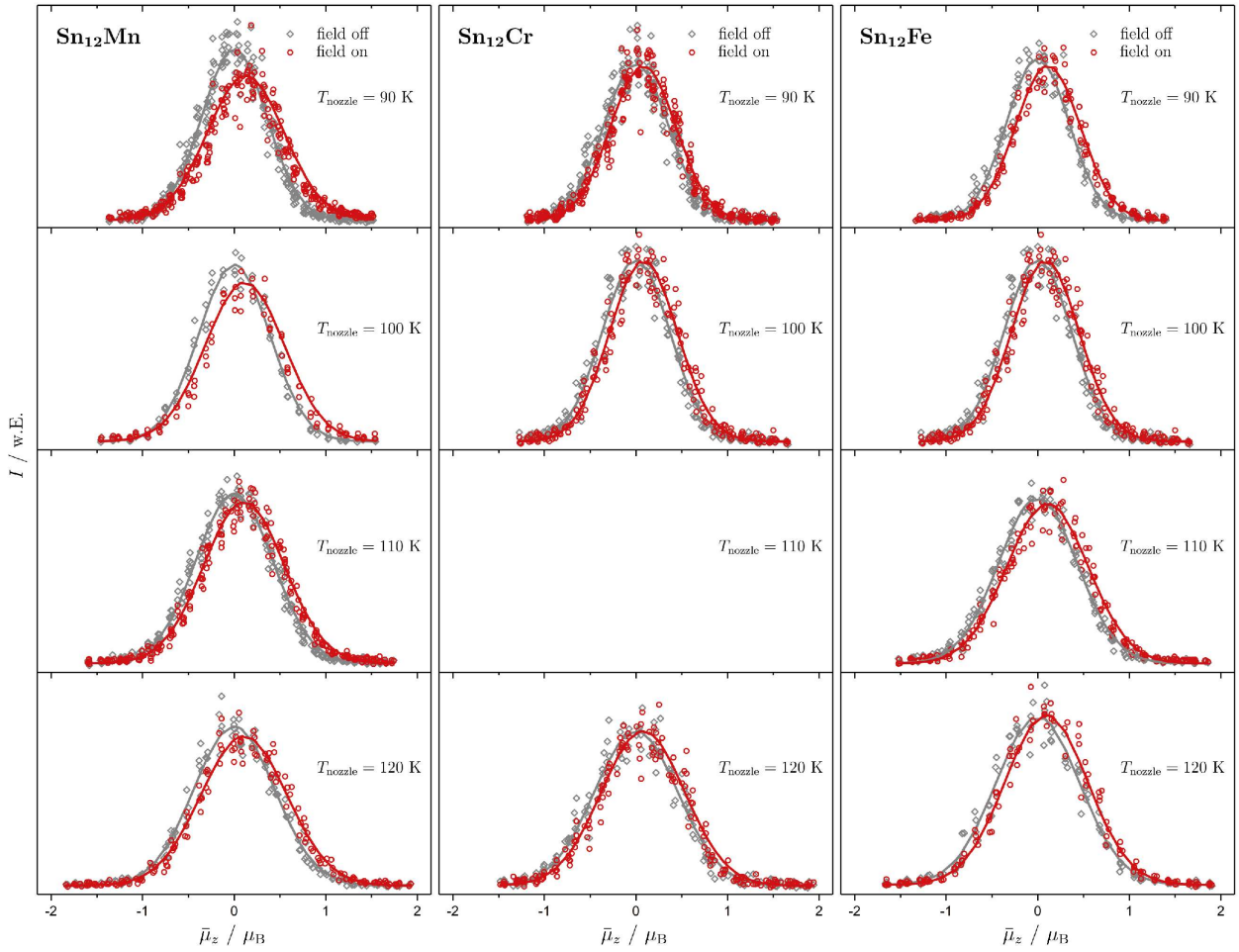

Figure S2. Magnetic deflection profiles of $Sn_{12}TM$ with TM = Mn, Cr and Fe (left to right) at $T_{nozzle} = 90 - 120$ K without (grey) and with (red) applied magnetic field. Gaussian functions are fitted to the experimental data. From the single-sided shift of this fit function, the g-factor and the Spin multiplicity S is determined in the main text with Curie's law. No deflection experiment was carried out for $Sn_{12}Cr$ at $T_{nozzle} = 110$ K. Please note that beam profiles get wider with increased temperature, since the beam width depends on the cluster velocity which increases with increasing T_{nozzle}.

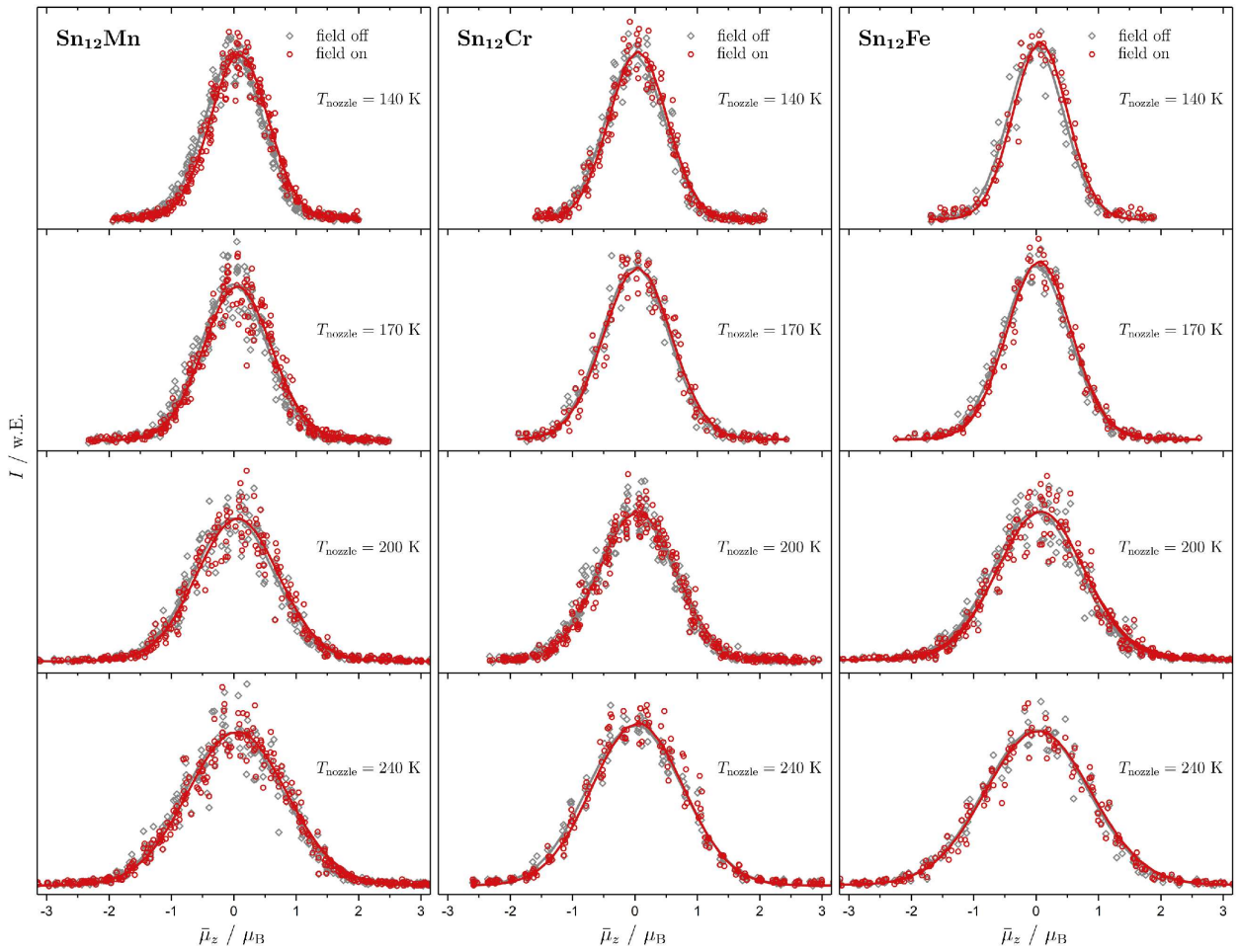

Figure S3. Magnetic deflection profiles of $Sn_{12}TM$ with TM = Mn, Cr and Fe (left to right) at $T_{\mathrm{nozzle}} = 140 - 240$ K without (grey) and with (red) applied magnetic field. Gaussian functions are fitted to the experimental data. From the single-sided shift of this fit function, the g-factor and the Spin multiplicity S is determined in the main text with Curie's law. Please note that beam profiles get wider with increased temperature, since the beam width depends on the cluster velocity which increases with increasing T_{nozzle}.

3 CASSCF Results for the g-factor

Table S1. Results for the g-factor of $Sn_{12}Cr$, $Sn_{12}Mn$ and $Sn_{12}Fe$. The table shows the three components of the g-factor, its isotropic value and the number of excited states considered for the calculation (roots). If no CAS size is given in parentheses, the values given are the result of calculations with an active space of 14 orbitals. The default basis set is (SARC)-DKH-TZVP.

	g_1	g_2	g_3	g_{iso}	Roots
$CrSn_{12}$ (14,10)	0.53	1.15	1.37	1.00	15
$CrSn_{12}$	1.92	1.93	2.00	1.95	5
$CrSn_{12}$	1.69	1.72	1.78	1.73	25
$CrSn_{12}$	1.70	1.72	1.81	1.74	45
$CrSn_{12}$	1.81	1.82	1.83	1.82	60
$CrSn_{12}$	1.87	1.88	1.88	1.88	80
$MnSn_{12}$ (I_h) (15,10)	2.01	2.04	2.04	2.03	15
$MnSn_{12}$ (I_h)	1.77	1.86	1.91	1.85	30
$MnSn_{12}$ (I_h)	1.75	1.75	1.75	1.75	40
$MnSn_{12}$ (I_h)	1.84	1.87	1.92	1.88	50
$MnSn_{12}$ (I_h)	1.93	1.93	1.93	1.93	60
$MnSn_{12}$ (T_h)	1.89	1.89	1.89	1.89	60
$MnSn_{12}$ (D_{5d})	1.91	1.92	1.92	1.92	60
$MnSn_{12}$ (D_{3d})	1.94	1.94	1.95	1.94	60
$MnSn_{12}$ (D_{2h})	1.91	1.91	1.92	1.92	60
$FeSn_{12}$ (16,10)	2.11	2.21	2.69	2.34	15
$FeSn_{12}$ (16,10) QZVPP - Fe	2.12	2.23	2.69	2.34	15
$FeSn_{12}$ (16,10)	2.25	2.35	2.69	2.43	30
$FeSn_{12}$ (16,10) QZVPP - Fe	2.24	2.37	2.68	2.43	30
$FeSn_{12}$	2.00	2.38	2.66	2.35	5
$FeSn_{12}$	2.15	2.46	2.71	2.44	30
$FeSn_{12}$ state-averaged	2.26	2.32	2.72	2.43	30,15,15
$FeSn_{12}$	2.19	2.47	2.68	2.45	45
$FeSn_{12}$	2.06	2.43	2.45	2.31	60

4 CASSCF Orbitals and Corresponding Excited States

In the following section the CASSCF orbitals from the active spaces mentioned in the main text are displayed. The orbitals are grouped as described in the main text and labeled according to the configurations shown in the following tables. For an example, the groundstate configuration of $Sn_{12}Mn$ is 22222 11111 0000. This means that the orbitals 1 to 5 are doubly occupied, the orbitals 6 to 10 are singly occupied and the orbitals 11 to 14 are unoccupied in this configuration. This is the same for $Sn_{12}Cr$ and $Sn_{12}Fe$. The tables show the most dominant configuration of the respective excited state sorted by their CASSCF energy. For $Sn_{12}Fe$ and $Sn_{12}Cr$ the low energy excited states are presented with the second most dominant configuration to emphasize their difference.

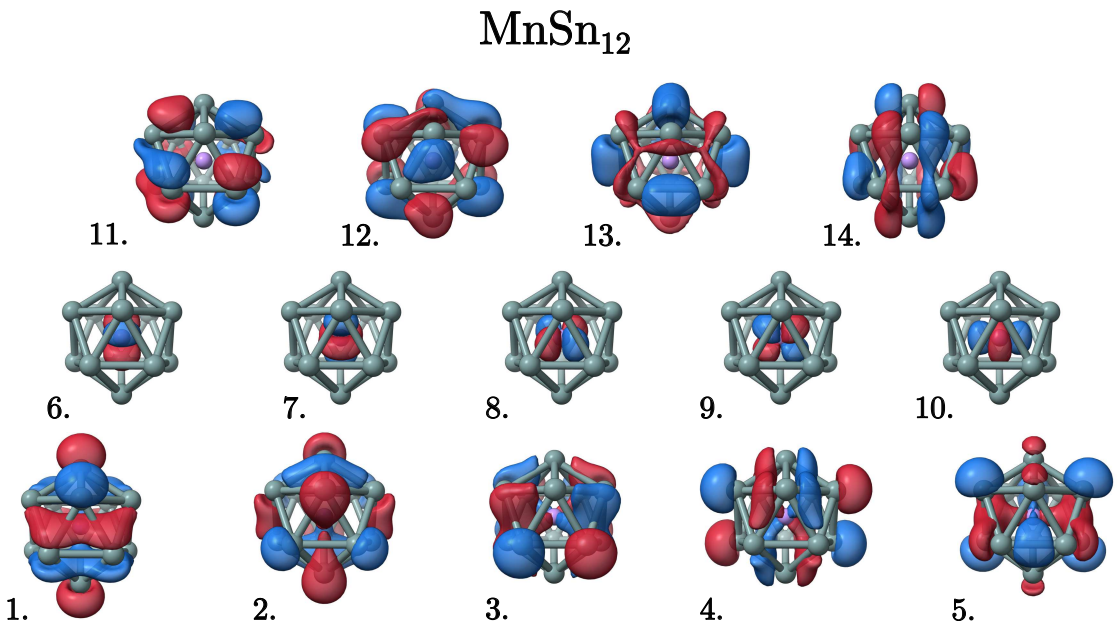

Figure S4. Active orbitals of $Sn_{12}Mn$ in the CAS(15,14) calculation. The orbitals are in the order of the configurations shown in the tables below and grouped as described in the main text.

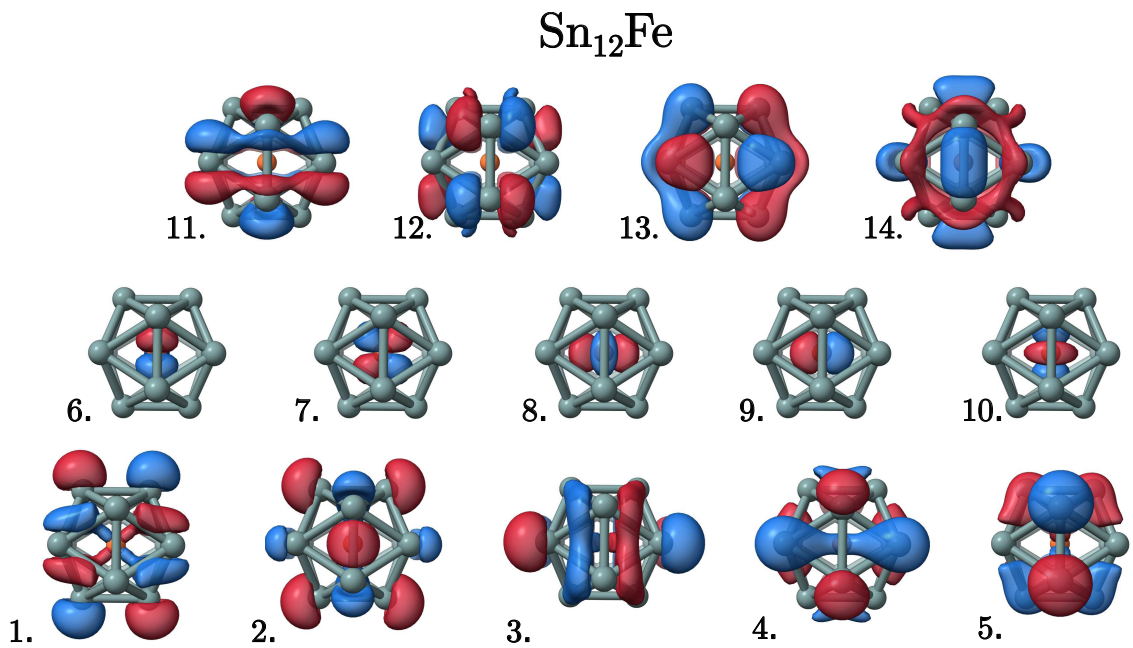

Figure S5. Active orbitals of $Sn_{12}Fe$ in the CAS(16,14) calculation. The orbitals are in the order of the configurations shown in the tables below and grouped as described in the main text.

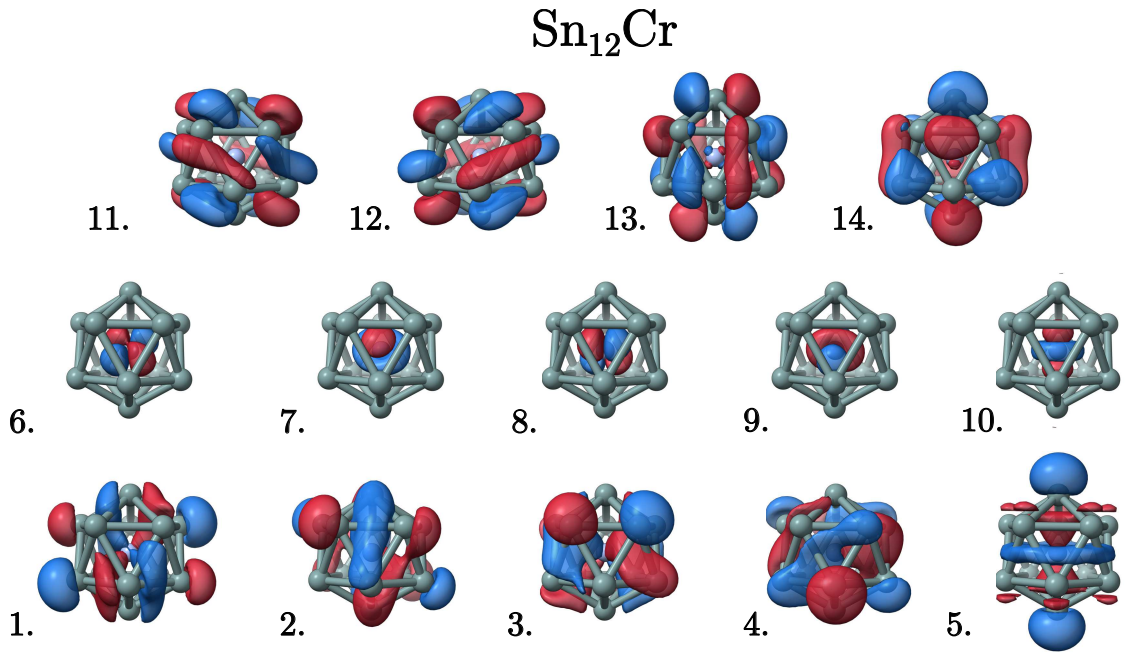

Figure S6. Active orbitals of $Sn_{12}Cr$ in the CAS(14,14) calculation. The orbitals are in the order of the configurations shown in the tables below and grouped as described in the main text.

Table S2. Excited states of $Sn_{12}Mn$ in I_h symmetry. The excited states are sorted by their CASSCF energy. The occupation in the electronic configuration matches the ordering of the active orbitals presented above.

Root	E(CASSCF)	E(NEVPT2)	Weight	Configuration
0	0	0.0	0.75	22222 11111 0000
1	17531.3	26459.9	0.72	22221 11211 0000
2	17538.2	26655.9	0.49	22221 11112 0000
3	17549.6	26387.9	0.5	22212 12111 0000
4	17557.4	26510.8	0.42	22212 21111 0000
5	17566.8	26635.2	0.23	21222 21111 0000
6	17579.8	26511.2	0.39	21222 11121 0000
7	17635.8	26498.8	0.3	12222 12111 0000
8	17653.5	26686.9	0.39	22221 12111 0000
9	17675.9	26638.1	0.38	22122 11112 0000
10	17677.7	26672.8	0.31	12222 11211 0000
11	17690.1	26739.4	0.29	22212 11211 0000
12	17694.8	26574.1	0.48	21222 12111 0000
13	17904.9	27034.1	0.36	22212 11112 0000
14	17918.9	27059.8	0.35	22212 11121 0000
15	17923.7	26829.0	0.54	22221 21111 0000
16	17958.9	26950.9	0.61	22122 12111 0000
17	17964.0	26988.0	0.33	12222 21111 0000
18	17986.2	26890.1	0.42	21222 11121 0000
19	18014.1	26901.1	0.61	12222 11112 0000
20	18022.3	26958.2	0.5	21222 11211 0000
21	18081.3	26926.1	0.27	22212 11211 0000
22	18082.5	26718.1	0.61	21222 11112 0000
23	18084.8	26901.1	0.36	22122 21111 0000
24	18114.5	26911.7	0.37	12222 11121 0000
25	19756.6	12600.2	0.59	22212 11111 0100
26	19777.0	12576.7	0.4	22221 11111 1000
27	19786.8	12604.3	0.37	22122 11111 1000
28	19792.2	12933.9	0.38	22221 11111 0100
29	19901.6	13002.7	0.26	22221 11111 0010
30	20109.3	12632.8	0.26	22122 11111 0100
31	20146.4	12905.2	0.27	21222 11111 0010
32	20219.0	12584.3	0.38	22122 11111 0010
33	20467.8	12567.2	0.26	21222 11111 0100
34	20511.8	12786.8	0.23	22212 11111 0010
35	20715.4	12873.4	0.15	21222 11111 0001
36	20720.8	12849.4	0.16	21222 11111 0001
37	20909.4	13125.4	0.17	22122 11111 0001
38	20956.7	12637.9	0.44	12222 11111 0001
39	21177.3	12786.0	0.28	21222 11111 0001
40	21434.5	13531.0	0.33	22122 11111 0100
41	21534.5	13474.1	0.31	22221 11111 0010
42	21903.1	13029.4	0.41	22221 11111 0001
43	22010.8	13068.7	0.39	22122 11111 0001
44	22041.7	13008.5	0.47	22212 11111 0001
45	25273.9	14568.4	0.64	22212 11111 0100
46	25288.1	14624.4	0.27	22122 11111 1000
47	25303.7	14576.0	0.42	22221 11111 1000
48	25336.5	14978.4	0.34	22122 11111 1000
49	25448.9	14980.0	0.31	22212 11111 1000
50	25654.1	15043.2	0.32	12222 11111 0100
51	25667.5	14920.8	0.26	22122 11111 0100
52	25788.8	14757.4	0.53	22122 11111 0010
53	25923.7	14989.1	0.37	22212 11111 0010
54	26051.3	15204.6	0.33	21222 11111 0100
55	26077.2	14737.2	0.47	12222 11111 0010
56	26273.2	14599.8	0.29	21222 11111 0001
57	26361.4	15090.2	0.39	22122 11111 0001
58	26374.0	14536.5	0.59	12222 11111 0001
59	26587.2	14710.9	0.34	21222 11111 0001

Table S3. Excited states of $Sn_{12}Mn$ in I_h symmetry for the CAS(15,10). The excited states are sorted by their CASSCF energy.

Root	E(CASSCF)	E(NEVPT2)	Weight	Configuration
0	0	0.0	0.59	22222 11111
1	15327.3	23726.4	0.77	21222 21111
2	15356.0	23949.6	0.65	12222 21111
3	15412.2	24121.0	0.49	22122 21111
4	15493.9	24255.3	0.39	22212 21111
5	15518.0	24216.0	0.47	22122 12111
6	15555.1	24112.4	0.58	22221 21111
7	15596.8	24293.6	0.44	22122 11211
8	15730.1	24313.7	0.51	22212 12111
9	15819.1	24493.3	0.26	12222 12111
10	15845.7	24407.7	0.37	22212 11211
11	15896.5	24584.6	0.34	21222 12111
12	15958.5	24302.9	0.49	21222 11211
13	16023.4	24458.6	0.35	22221 12111
14	16041.2	24417.6	0.38	22122 11211

Table S4. Excited states of $Sn_{12}Fe$ in D_{2h} symmetry. The excited states are sorted by their CASSCF energy. The occupation in the electronic configuration matches the ordering of the active orbitals presented above.

Root	E(CASSCF)	E(NEVPT2)	Weight	Configuration
0	0	0.0	0.4	22222 21111 0000
			0.18	22212 21211 0000
1	0.6	221.1	0.31	22222 11211 0000
			0.18	22221 21211 0000
2	93.4	460.4	0.42	22222 12111 0000
			0.15	22221 22111 0000
3	253.9	362.7	0.42	22222 11121 0000
			0.16	21222 11122 0000
4	335.0	447.2	0.32	22222 11112 0000
			0.15	22212 11212 0000
5	7643.1	12203.5	0.33	22221 22111 0000
6	7715.2	12180.1	0.44	22212 22111 0000
7	7820.8	12312.0	0.46	22212 21211 0000
8	7823.8	12383.7	0.4	22221 21211 0000
9	7856.4	12169.7	0.92	22221 11212 0000
10	7876.0	12353.5	0.44	22221 12211 0000
11	7906.6	12324.6	0.74	22122 21211 0000
12	7963.0	12565.4	0.66	22221 12121 0000
13	7972.7	12642.2	0.41	22212 21121 0000
14	8057.2	12653.0	0.67	22212 12121 0000
15	8059.1	12455.8	0.79	22221 11122 0000
16	8209.3	12500.3	0.7	21222 21211 0000
17	8224.9	12846.9	0.19	22221 21121 0000
18	8291.6	12918.5	0.24	22212 12211 0000
19	8317.5	12909.2	0.68	22212 11122 0000
20	8367.7	13169.3	0.36	22122 22111 0000
21	8431.1	13184.1	0.34	22212 11212 0000
22	8480.7	13225.0	0.37	22122 11212 0000
23	8499.1	12929.5	0.72	21222 21121 0000
24	8515.5	13081.7	0.51	22122 12211 0000
25	8596.4	13301.8	0.53	22122 11212 0000
26	8782.5	13479.0	0.41	21222 12211 0000
27	8793.1	13450.6	0.39	21222 12121 0000
28	8974.5	12463.5	0.83	12222 21211 0000
29	9018.2	13313.2	0.41	12222 22111 0000
30	9177.3	13504.3	0.33	12222 12211 0000
31	9346.0	13672.7	0.48	12222 12121 0000
32	9390.3	13645.8	0.36	12222 21121 0000
33	9610.9	13351.9	0.94	12222 11212 0000
34	9812.3	13612.2	0.91	12222 11122 0000
35	17160.2	6021.6	0.11	22221 21111 1000
36	17332.8	6179.2	0.12	22221 21111 0100
37	17688.1	6461.5	0.11	22221 21111 0010
38	18009.8	6904.9	0.11	22221 21111 0001
39	19732.4	17171.6	0.28	22221 21112 0000
40	19843.3	16967.9	0.26	22212 11221 0000
41	19850.6	15757.5	0.13	22221 11221 0000
42	19939.4	10640.4	0.18	22212 11211 1000
43	19951.3	10480.1	0.29	22221 11112 0100
44	19981.0	10653.2	0.12	22221 21111 0100
45	20027.0	10680.8	0.23	22212 12111 1000
46	20032.5	10931.2	0.2	22221 12111 0100
47	20071.0	11678.3	0.15	22212 21111 1000
48	20099.1	12823.0	0.1	22122 11211 1000
49	20113.2	11314.6	0.16	22221 11121 0100
50	20151.5	11217.3	0.11	22122 11211 1000
51	20189.2	13614.6	0.08	21222 21112 0000
52	20196.1	11842.1	0.16	22221 11211 0100
53	20259.3	10641.2	0.22	22122 21111 1000
54	20288.9	14661.4	0.1	21222 21112 0000
55	20317.1	11216.5	0.17	22221 11112 1000
56	20376.9	10772.7	0.11	22212 11112 1000
57	20386.5	16171.1	0.16	22122 11221 0000
58	20463.7	10916.3	0.17	22212 11211 0100
59	20472.5	11717.2	0.11	22212 21111 1000

Table S5. Excited states of $Sn_{12}Fe$ in D_{2h} symmetry for the CAS(16,10) active space. The excited states are sorted by their CASSCF energy.

Root	E(CASSCF)	E(NEVPT2)	Weight	Configuration
0	0	236.2	0.32	22222 12111
			0.20	22221 22111
1	3.8	0.0	0.4	22222 21111
			0.21	22212 22111
2	116.1	502.6	0.42	22222 11211
			0.16	22221 21211
3	300.2	427.7	0.41	22222 11121
			0.17	22221 21121
4	371.1	511.0	0.32	22222 11112
			0.15	22212 12112
5	7833.5	12109.8	0.37	22212 21121
6	7911.0	12055.6	0.47	22212 21211
7	7944.9	12157.6	0.54	22212 22111
8	7991.0	12225.4	0.48	22221 22111
9	8036.3	12084.7	0.82	22122 22111
10	8059.2	12075.4	0.93	22221 12112
11	8169.1	12622.9	0.33	22212 21121
12	8172.9	12298.9	0.48	22221 11212
13	8265.6	12518.4	0.69	22221 11221
14	8273.0	12265.3	0.78	22221 11122
15	8292.3	12649.2	0.5	22212 11221
16	8375.3	12533.2	0.52	21222 22111
17	8459.0	12867.8	0.21	22221 21121
18	8504.0	12794.1	0.78	22212 11122
19	8551.1	12959.6	0.28	22122 11221
20	8577.8	13089.1	0.35	22212 12112
21	8632.4	13039.3	0.4	22122 21211
22	8642.9	12990.3	0.36	22122 12112
23	8729.5	12760.7	0.71	21222 21121
24	8730.5	12987.3	0.38	22122 12211
25	8738.6	12432.6	0.69	12222 22111
26	8792.3	13149.0	0.49	22122 12112
27	8905.7	13131.6	0.3	12222 21211
28	9092.3	13297.7	0.43	21222 12211
29	9121.1	13047.5	0.6	12222 21121

Table S6. Excited states of $Sn_{12}Cr$ in D_{5d} symmetry. The excited states are sorted by their CASSCF energy. The occupation in the electronic configuration matches the ordering of the active orbitals presented above.

Root	E(CASSCF)	E(NEVPT2)	Weight	Configuration
0	0	0.0	0.84	22222 11110 0000
1	837.0	1060.8	0.56	22222 11101 0000
			0.29	22222 10111 0000
2	849.0	1094.2	0.57	22222 11011 0000
			0.27	22222 01111 0000
3	1073.5	1384.8	0.56	22222 10111 0000
			0.28	22222 11101 0000
4	1077.5	1380.8	0.58	22222 01111 0000
			0.27	22222 11011 0000
5	13593.0	6744.8	0.1	22222 11100 1000
6	13769.0	6585.7	0.22	22222 11010 1000
7	13789.9	6677.2	0.24	22222 11100 0100
8	13916.7	6839.5	0.14	22222 10110 1000
9	14473.3	7296.5	0.08	22222 11010 0010
10	14483.0	7262.5	0.07	22222 10110 1000
11	14562.3	7458.2	0.09	22222 11010 0100
12	14605.8	7535.0	0.09	22222 01110 1000
13	14806.8	7857.3	0.21	22222 11010 0010
14	14830.4	7870.8	0.2	22222 11100 0010
15	15001.9	7959.4	0.13	22222 11010 0001
16	15052.6	7953.6	0.12	22222 11100 0001
17	15218.7	8112.6	0.29	22222 10110 0001
18	15297.7	8044.0	0.23	22222 01110 0001
19	15322.0	8083.6	0.37	22222 01110 0010
20	15339.1	8012.7	0.3	22222 10110 0010
21	15685.8	8085.7	0.31	22222 11001 1000
22	15690.9	8098.7	0.31	22222 11001 0100
23	15848.6	8272.4	0.19	22222 10101 1000
24	15861.7	8285.6	0.19	22222 10101 0100
25	16130.8	8152.0	0.28	22222 00111 1000
26	16141.5	8157.9	0.28	22222 00111 0100
27	16689.7	8728.3	0.1	22222 11001 0010
28	16755.1	8593.6	0.04	22222 10101 1000
29	16985.4	8575.7	0.11	22222 01101 0100
30	16994.1	8552.7	0.12	22222 10011 1000
31	17137.3	9085.4	0.24	22222 11001 0010
32	17328.5	9342.5	0.17	22222 00111 0001
33	17572.8	9418.3	0.25	22222 11001 0001
34	17656.1	9597.1	0.18	22222 01011 0001
35	17715.8	9597.5	0.14	22222 00111 0001
36	17861.7	9505.4	0.33	22222 00111 0010
37	18066.6	9319.8	0.16	22222 10011 0100
38	18067.3	9311.8	0.16	22222 01101 1000
39	18582.2	9920.2	0.08	22222 01011 0010
40	18603.5	9995.9	0.09	22222 10101 0001
41	18763.6	10086.5	0.07	22222 01101 0010
42	18772.6	10097.0	0.06	22222 10011 0001
43	19902.9	10616.0	0.14	22222 10011 0001
44	19922.1	10615.0	0.13	22222 01101 0010
45	22905.9	13764.3	0.62	22221 11110 1000
46	22911.6	13781.9	0.61	22221 11110 0100
47	22951.3	14023.0	0.76	22221 11110 0010
48	22956.5	13971.1	0.77	22221 11110 0001
49	23242.7	13820.0	0.57	22221 11011 0010
50	23257.8	13874.2	0.54	22221 11101 0010
51	23306.8	13964.7	0.35	22221 11101 0001
52	23323.4	14012.9	0.36	22221 01111 0001
53	23385.6	13788.6	0.51	22221 10111 0001
54	23496.8	13445.5	0.09	22221 11011 0100
55	23516.4	14293.1	0.41	22221 10111 0010
56	23530.7	13945.9	0.44	22221 01111 0010
57	23578.0	13293.1	0.14	22221 11011 1000
58	23651.5	13557.9	0.2	22221 11101 0100
59	23694.0	13541.2	0.14	22221 11011 0100

Table S7. Excited states 60 to 79 of $Sn_{12}Cr$ in D_{5d} symmetry. The excited states are sorted by their CASSCF energy. The occupation in the electronic configuration matches the ordering of the active orbitals presented above.

Root	E(CASSCF)	E(NEVPT2)	Weight	Configuration
60	23806.1	14366.5	0.26	22221 01111 0001
61	24075.3	13858.3	0.21	22221 10111 1000
62	24107.1	13818.4	0.45	22221 10111 0100
63	24126.0	13952.8	0.35	22221 01111 0100
64	24132.8	13888.8	0.47	22221 01111 1000
65	24807.1	15039.9	0.20	22212 11110 1000
66	25015.8	14953.5	0.43	22212 11110 0100
67	25018.6	14787.1	0.39	22122 11110 1000
68	25183.3	16706.3	0.46	22221 11110 0010
69	25223.8	17489.8	0.63	22221 11110 0001
70	25312.5	16399.4	0.28	22221 11110 0100
71	25333.6	16735.7	0.34	22221 11110 0100
72	25338.5	16822.7	0.49	22221 11110 1000
73	25470.7	14847.8	0.18	22212 11011 0100
74	25483.9	14848.4	0.20	22122 11101 1000
75	25717.2	15218.2	0.06	21222 11110 1000
76	25732.8	15142.9	0.12	22212 11011 0100
77	25770.5	15063.0	0.24	22122 01111 1000
78	25786.6	15210.2	0.12	22212 10111 0100
79	25863.8	15474.3	0.15	21222 11110 0100

Table S8. Excited states of $Sn_{12}Cr$ in D_{5d} symmetry for the CAS(14,10) active space. The excited states are sorted by their CASSCF energy.

Root	E(CASSCF)	E(NEVPT2)	Weight	Configuration
0	0	75.9	0.54	22221 11111
1	1898.9	0.0	0.44	12222 11111
2	1898.9	20.2	0.44	21222 11111
3	1991.1	137.8	0.54	22212 11111
4	2023.8	91.5	0.54	22122 11111
5	18290.8	11102.6	0.43	22221 11111
6	19143.3	12042.0	0.41	22212 11111
7	19178.2	12038.1	0.4	22122 11111
8	19425.6	12773.3	0.38	12222 11111
9	19425.7	12791.8	0.38	21222 11111
10	27486.1	21541.6	0.5	22221 11102
11	27486.2	21531.0	0.97	22221 11111
12	27543.9	21578.1	0.16	22221 12110
13	27544.5	21566.7	0.16	22221 11210
14	27915.8	21860.7	0.22	22221 12011

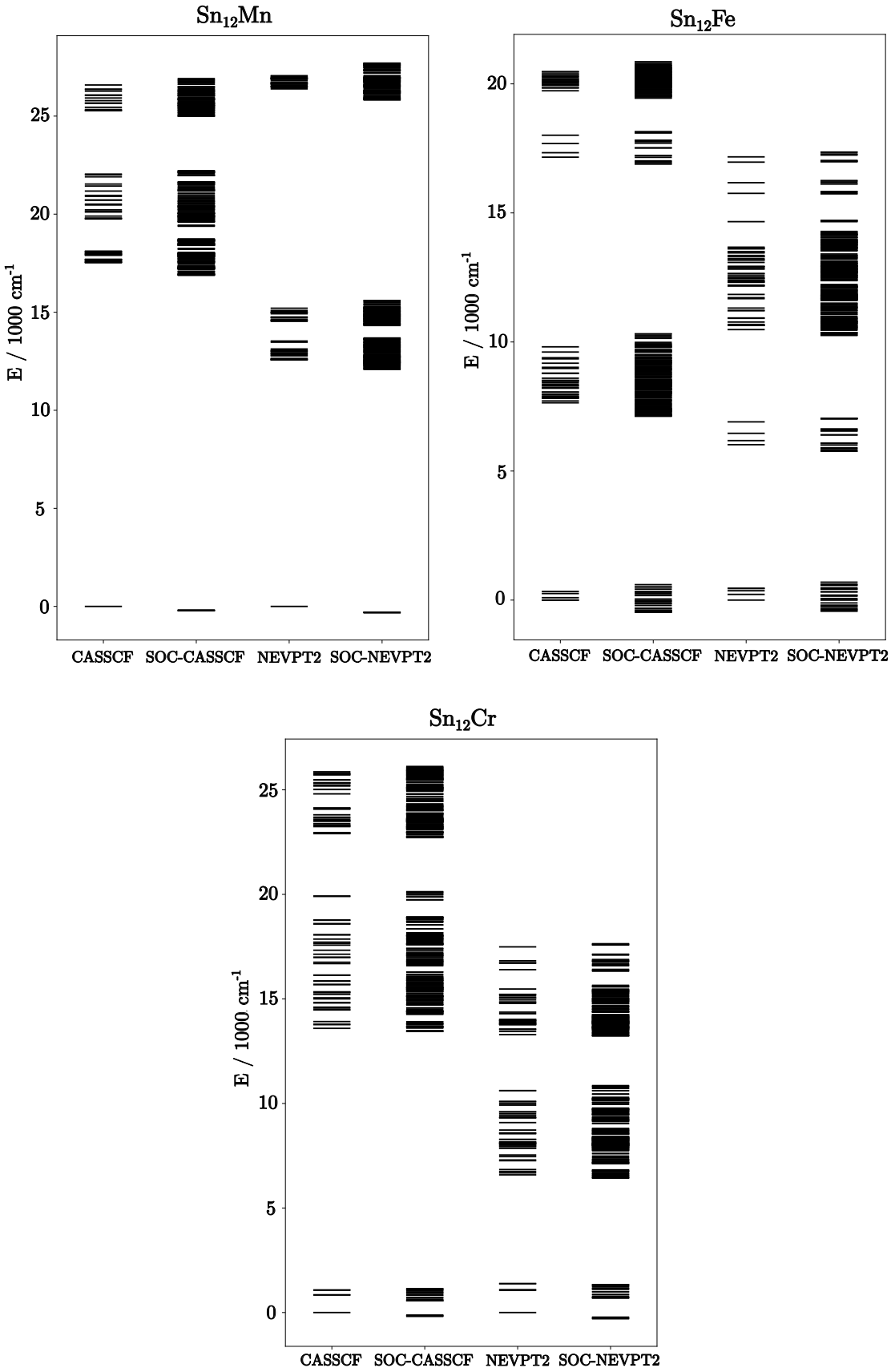

Figure S7. Energy levels of the ground and excited states of a) $Sn_{12}Mn$ b) $Sn_{12}Fe$ and c) $Sn_{12}Cr$ at different levels of theory, indicated on the bottom of the plot. The active space always contains the 14 orbitals as shown above and the calculations are done with the (SARC)-DKH-TZVP basis set.

5 Geometric structures

Table S9. Cartesian coordinates of $Sn_{12}Mn$ in I_h symmetry in in Angstroms.

Mn	-0.000006000000	0.000074000000	0.000001000000
Sn	1.662298000000	1.424738000000	2.158053000000
Sn	1.547861000000	2.504003000000	-0.886672000000
Sn	-1.182520000000	0.047671000000	2.837112000000
Sn	-3.055104000000	0.275164000000	0.212239000000
Sn	-1.367523000000	1.793062000000	-2.089212000000
Sn	-1.070726000000	2.703509000000	0.998026000000
Sn	1.071064000000	-2.703385000000	-0.997861000000
Sn	1.367084000000	-1.793415000000	2.089276000000
Sn	3.055029000000	-0.275207000000	-0.212019000000
Sn	1.182573000000	-0.047564000000	-2.837024000000
Sn	-1.547911000000	-2.503812000000	0.886318000000
Sn	-1.662122000000	-1.424801000000	-2.158237000000

Table S10. Cartesian coordinates of $Sn_{12}Mn$ in D_{2h} symmetry in in Angstroms.

Mn	0.000000000	0.000000000	0.000000000
Sn	-1.614451008	0.000000000	2.584331317
Sn	0.000000000	2.632180353	1.593247014
Sn	-2.615038889	-1.638721192	0.000000000
Sn	-1.614451008	0.000000000	-2.584331317
Sn	0.000000000	2.632180353	-1.593247014
Sn	-2.615038889	1.638721192	0.000000000
Sn	2.615038889	-1.638721192	0.000000000
Sn	0.000000000	-2.632180353	1.593247014
Sn	1.614451008	0.000000000	2.584331317
Sn	2.615038889	1.638721192	0.000000000
Sn	0.000000000	-2.632180353	-1.593247014
Sn	1.614451008	0.000000000	-2.584331317

Table S11. Cartesian coordinates of $Sn_{12}Mn$ in D_{3d} symmetry in in Angstroms.

Mn	0.000000000	0.000000000	0.000000000
Sn	-1.599544557	-0.923497481	2.458261468
Sn	1.599544557	-0.923497481	2.458261468
Sn	-2.622016723	1.513822061	0.585406370
Sn	0.000000000	3.027644121	-0.585406370
Sn	2.622016723	1.513822061	0.585406370
Sn	0.000000000	1.846994962	2.458261468
Sn	0.000000000	-1.846994962	-2.458261468
Sn	-2.622016723	-1.513822061	-0.585406370
Sn	0.000000000	-3.027644121	0.585406370
Sn	2.622016723	-1.513822061	-0.585406370
Sn	-1.599544557	0.923497481	-2.458261468
Sn	1.599544557	0.923497481	-2.458261468

Table S12. Cartesian coordinates of $Sn_{12}Mn$ in D_{5d} symmetry in in Angstroms.

Mn	0.000000000	0.000000000	0.000000000
Sn	-2.614542897	-0.849516484	1.389528125
Sn	-1.615876376	2.224063029	1.389528125
Sn	-1.615876376	-2.224063029	-1.389528125
Sn	0.000000000	0.000000000	-3.032676209
Sn	0.000000000	2.749093090	-1.389528125
Sn	-2.614542897	0.849516484	-1.389528125
Sn	2.614542897	-0.849516484	1.389528125
Sn	0.000000000	-2.749093090	1.389528125
Sn	0.000000000	0.000000000	3.032676209
Sn	1.615876376	2.224063029	1.389528125
Sn	1.615876376	-2.224063029	-1.389528125
Sn	2.614542897	0.849516484	-1.389528125

Table S13. Cartesian coordinates of $Sn_{12}Mn$ in T_h symmetry in in Angstroms.

Mn	0.000000000	0.000000000	0.000000000
Sn	0.000000000	-1.597922819	-2.578508528
Sn	-2.578508528	0.000000000	-1.597922819
Sn	2.578508528	0.000000000	-1.597922819
Sn	1.597922824	2.578508536	0.000000000
Sn	-1.597922815	2.578508521	0.000000000
Sn	0.000000000	1.597922819	-2.578508528
Sn	0.000000000	-1.597922819	2.578508528
Sn	1.597922815	-2.578508521	0.000000000
Sn	-1.597922824	-2.578508536	0.000000000
Sn	-2.578508528	0.000000000	1.597922819
Sn	2.578508528	0.000000000	1.597922819
Sn	0.000000000	1.597922819	2.578508528

Table S14. Cartesian coordinates of $Sn_{12}Fe$ in D_{2h} symmetry in in Angstroms.

Fe	0.000007000000	0.000024000000	-0.000024000000
Sn	-0.026669000000	2.544849000000	1.558700000000
Sn	-2.568220000000	1.564311000000	-0.007629000000
Sn	-0.017663000000	2.544082000000	-1.560014000000
Sn	-1.581052000000	-0.013086000000	2.497370000000
Sn	2.540563000000	1.608784000000	0.006799000000
Sn	1.566374000000	0.014296000000	2.506185000000
Sn	2.568216000000	-1.564315000000	0.007624000000
Sn	-2.540559000000	-1.608780000000	-0.006803000000
Sn	-1.566372000000	-0.014303000000	-2.506194000000
Sn	0.026663000000	-2.544860000000	-1.558666000000
Sn	1.581055000000	0.013077000000	-2.497378000000
Sn	0.017660000000	-2.544067000000	1.560019000000

Table S15. Cartesian coordinates of $Sn_{12}Cr$ in D_{5d} symmetry in in Angstroms.

Cr	0.000000000000	0.000003000000	-0.000019000000
Sn	-0.000007000000	0.000002000000	2.909545000000
Sn	0.852758000000	-2.547124000000	1.352624000000
Sn	-2.158970000000	-1.598134000000	1.352620000000
Sn	2.686004000000	0.023908000000	1.352611000000
Sn	-2.187078000000	1.559459000000	1.352624000000
Sn	0.807286000000	2.561905000000	1.352633000000
Sn	-0.852759000000	2.547128000000	-1.352623000000
Sn	2.187082000000	-1.559460000000	-1.352622000000
Sn	-0.807288000000	-2.561908000000	-1.352629000000
Sn	0.000006000000	-0.000008000000	-2.909563000000
Sn	-2.686011000000	-0.023909000000	-1.352601000000
Sn	2.158976000000	1.598138000000	-1.352609000000

6 Density of states plots

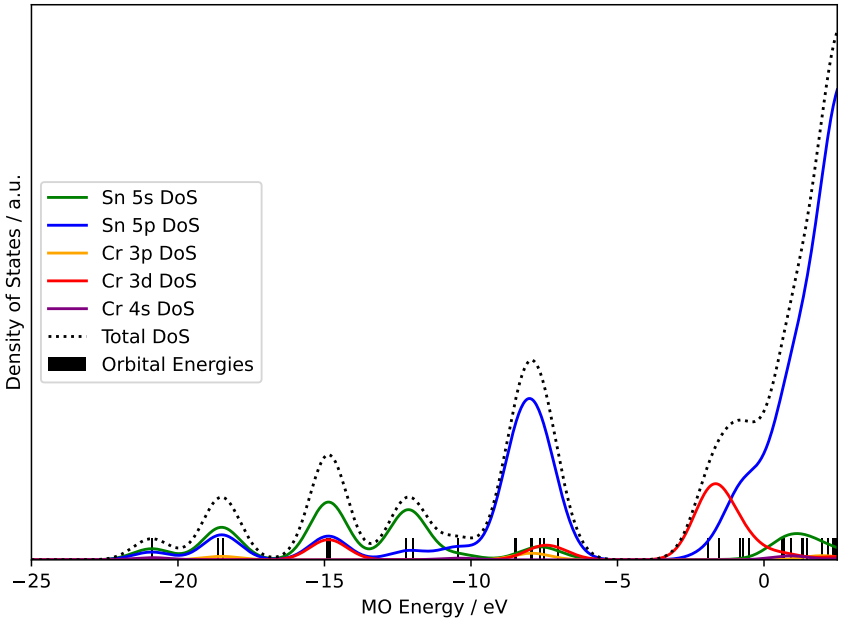

Figure S8. Density of states plot for $Sn_{12}Cr$ based on Löwdin orbital compositions which are obtained from ORCA. To obtain the plot, every MO energy is convoluted with a Gaussian of $\sigma^2 = 0.4$ eV.

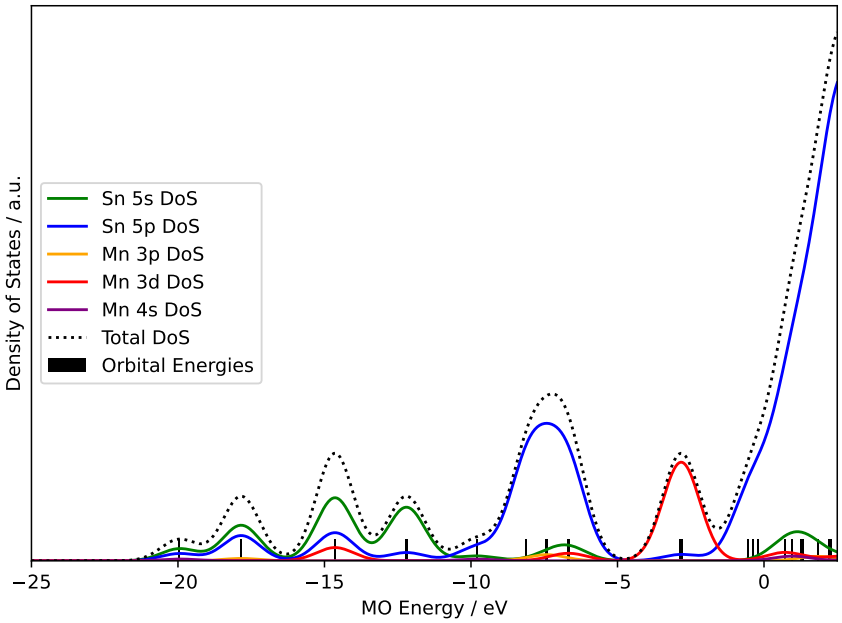

Figure S9. Density of states plot for $Sn_{12}Mn$ based on Löwdin orbital compositions which are obtained from ORCA. To obtain the plot, every MO energy is convoluted with a Gaussian of $\sigma^2 = 0.4$ eV.

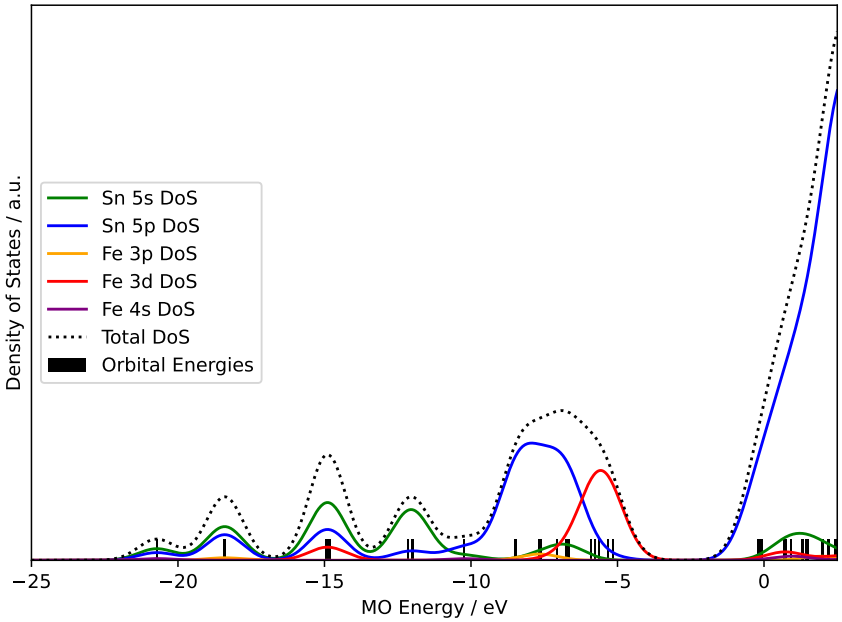

Figure S10. Density of states plot for $Sn_{12}Fe$ based on Löwdin orbital compositions which are obtained from ORCA. To obtain the plot, every MO energy is convoluted with a Gaussian of $\sigma^2 = 0.4$ eV.